

The Design and Use of a Photochemical Flow Reactor: A Laboratory Study of the Atmospheric Chemistry of Cyanoacetylene on Titan

David W. Clarke,¹ Jeffrey C. Joseph, and James P. Ferris

Rensselaer Polytechnic Institute, Department of Chemistry, Troy, New York 12180

E-mail: ferrij@rpi.edu

Received September 20, 1999; revised April 4, 2000

The laboratory investigation of the atmospheric photochemistry of planets and satellites is mainly carried out in static systems. These studies are often poor models of chemical processes in atmospheres because: (1) much higher mixing ratios of minor constituents must be used to accurately determine the amount of reactant consumed and to obtain sufficient products for analysis, (2) secondary photolysis of the initial photoproducts often occurs, (3) wall reactions occur, and (4) most of the starting material is converted to products to obtain enough for spectroscopic analysis. The use of a photochemical flow reactor either circumvents or minimizes these problems by using gas mixtures and photolysis conditions more representative of a planetary atmosphere. A gas mixture, composed of a small amount of a reactant gas diluted in a much larger amount of carrier gas, is flowed past a UV lamp for an extended period of time. Unconsumed reactants and products are collected in traps downstream until amounts sufficient for spectral analysis are collected. FTIR and NMR analysis provides structural information and quantitative data on their rates of formation.

The feasibility of this approach for the investigation of planetary atmospheres has been demonstrated by the photolysis of mixing ratios of 10^{-3} – 10^{-6} of cyanoacetylene, (2-propynenitrile, HC_3N) in nitrogen gas. Hydrogen cyanide (HCN), acetonitrile (CH_3CN), acrylonitrile (CH_2CHCN), and a polymer have been identified as reaction products. The quantum yields for reactant loss and product formation have been determined. Aspects of polymer structure have been determined by FTIR. Its empirical formula has been determined on the basis of the reaction products produced, and its morphology has been examined by scanning electron microscopy. It is concluded from the high quantum yields for HCN and CH_3CN formation that the C/N ratio of the polymer is high. This was confirmed by infrared analysis of the polymer where it was observed that the intensity of the $\text{C}\equiv\text{N}$ stretching frequency decreases as the HC_3N mixing ratio is lowered to a mixing ratio closer to that of Titan. © 2000 Academic Press

Key Words: atmospheres; evolution; photochemistry; prebiotic chemistry; radiation chemistry; Titan.

INTRODUCTION

Titan, the largest moon of Saturn, captured the interest of astronomers and atmospheric scientists alike when methane (CH_4) (Kuiper 1944) was discovered in its 1.5 bar nitrogen (N_2) atmosphere. This interest has continued to grow as additional ground-based measurements and the Voyager I flyby in 1980 added other organics to the list of atmospheric constituents. Among those identified are a suite of saturated and unsaturated hydrocarbons, several nitriles, and small amounts of four oxygenated compounds. The presence of stratospheric haze layers suggests that the photochemistry of these minor constituents may be critical in understanding Titan's atmospheric chemistry even though their mixing ratios range from only 10^{-5} to 10^{-9} . Despite the low mixing ratio of water vapor (8×10^{-9}) (Coustenis *et al.* 1998) and the low temperatures present (≤ 160 K), the haze formation, coupled with the wide array of organics found, has fostered the opinion that Titan may be the best observable model of processes of chemical evolution similar to those that occurred on primitive Earth. Laboratory studies of the atmospheric processes occurring on Titan might also contribute to our understanding of the data returned from the Huygens probe of the Cassini Mission due to reach Titan in 2004.

One of the more interesting components of Titan's atmosphere is cyanoacetylene (2-propynenitrile, HC_3N). HC_3N is the third most prevalent nitrogen-containing compound in the atmosphere, after N_2 and HCN. Its light absorbing properties and photochemical reactivity also indicate that it could have an important role in the atmospheric chemistry on Titan (Clarke and Ferris 1996). HC_3N absorbs light at wavelengths as long as 260 nm (Job and King 1966a, 1966b) and is photoreactive at wavelengths out to at least 254 nm (Ferris and Guillemin 1990). As HC_3N has been identified as a precursor to the pyrimidines essential to the origin of life on Earth (Ferris *et al.* 1968, 1974), it is a molecule of prebiotic significance as well. Previous studies of HC_3N photochemistry have examined the primary processes that occur following irradiation, as well as secondary reactions (Halpern *et al.* 1990, 1988, 1989, Ferris and Guillemin 1990, Clarke and Ferris 1995, 1996, 1997b, Seki *et al.* 1996). However, in all of these studies the HC_3N pressure has been higher

¹ Current address: Albany College of Pharmacy, 106 New Scotland Ave., Albany, NY 12208. E-mail: clarked@panther.acp.edu. Fax: 518-445-7202.

than 0.01 Torr. While providing insight into the photochemical processes occurring, it is unknown how well this data can be extrapolated to the conditions on Titan, where the HC_3N mixing ratios range from 10^{-7} to 10^{-9} . The use of lower pressures in static systems (systems in which a sealed vessel containing reactants is irradiated) such as these is not practical as neither the small amount of reactant consumed nor the products formed can be determined with any degree of accuracy.

A flow system was designed to overcome the limitations of a static system by flowing small quantities of reactant in an inert carrier gas through a reaction zone for extended periods of time. Flow systems have been successfully utilized for the study of charged particle reactions under conditions similar to those expected in planetary atmospheres (Thompson *et al.* 1991, McDonald *et al.* 1994). Our work has concentrated on developing a flow system capable of examining photochemical processes in a variety of planetary atmospheres. The flow system and flow reactor photochemistry of HC_3N will be described in this report.

EXPERIMENTAL

A. The Flow System

System construction. The flow system is divided into three primary sections (Fig. 1). The first is a standard glass vacuum rack that allows for trace (reactant) gases to be introduced into the second section. In the second, stainless steel, section the reactant gas is mixed with a carrier gas. The gas mixture is then introduced into the third section using a mass flow controller, where the photochemistry is performed. After passing through the photolysis cell, gases are collected in cryogenic traps downstream. A restriction, situated before the traps, controls the operating pressure in the cell.

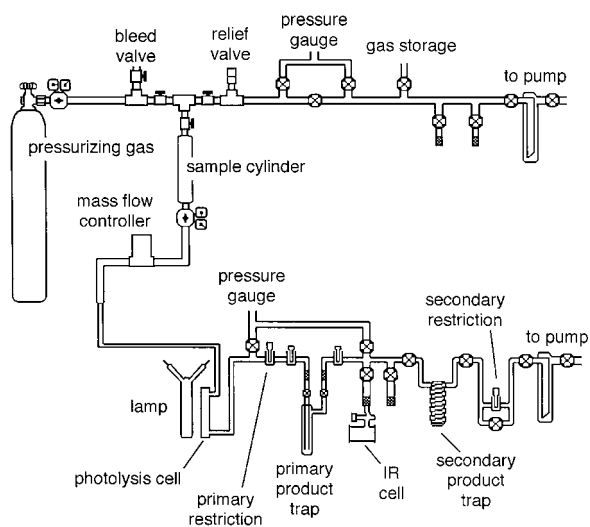


FIG. 1. Photochemical flow reactor.

TABLE I
Experiments for the Verification of Complete Mixing

Date of run	Run time (h)	HC_3N recovered (mol/s)
March 29	4	1.18×10^{-5}
March 31	8	1.18×10^{-5}
April 1	12	1.21×10^{-5}
April 11	2	1.23×10^{-5}

An oil diffusion pump and two Welch Model 1402 rough pumps evacuate the system. Pressure measurements of less than 1000 Torr are made by a MKS Baratron Model 390-HA1000 with a Model 270C Signal Conditioner. The initial pressure in the cylinder of the flow system (62,000 Torr) was measured with the regulator gauge with an error of ± 1500 Torr. Gas flow was controlled by a MKS 1159B Mass Flow Controller (0–100 standard $\text{cm}^3\text{min}^{-1}$ capacity) connected to a MKS Type 246B Single Channel Readout. The sample cylinder, for preparing gas mixtures for flow experiments, was constructed with 318 stainless steel valves and tubing capable of withstanding 1800 psi and holding $\sim 10^{-4}$ Torr vacuum.

Preparation of reactant gases. Reactant mixtures were prepared using N_2 as a carrier gas and had HC_3N mixing ratios varying from 10^{-3} to 10^{-6} . HC_3N was synthesized by the method of Moureau and Bongrand (1920) as modified by Miller and Lemmon (1967). The impurities present in the HC_3N were less than 0.03% as determined by ^1H NMR. ULSI grade N_2 (99.9999%) was used directly as obtained from Matheson. In order to prepare a mixture for photolysis, the system was evacuated and a measured amount of HC_3N was introduced into the sample cylinder. The stainless steel portion of the system was then isolated from the glass section and pressurized with N_2 . A typical mixture containing an HC_3N mixing ratio of 10^{-5} would be prepared by pressurizing 0.62 Torr of HC_3N with 1200 psi (62,000 Torr) of N_2 . As the precision of the mass flow controller and analysis methods was greater than that of the sample cylinder pressure gauge, control runs, in which no photolysis occurred, were used to determine the actual mixing ratios. These control runs were also used to determine if impurities were present in the starting gases used.

With such small quantities of reactant gases present, complete mixing is essential. An estimate of the time required was calculated by assuming a cylindrical sample compartment and that the gases are initially present as two separate layers (Eq. (1)) (Bamford and Tipper 1969). The times calculated for complete mixing are on the order of days. As some turbulence during pressurizing is expected, the gases will not start uniformly separated and actual mixing times should be significantly less than the calculated values. A series of control runs was performed over a period of two weeks to verify that complete mixing of the reactant gases occurs within this time frame (Table I). The variation in HC_3N recovered, expressed as a relative deviation,

is less than 3%,

$$t = \frac{3L^2}{4D} \quad D = \frac{3c}{32n\delta^2}, \quad (1)$$

where

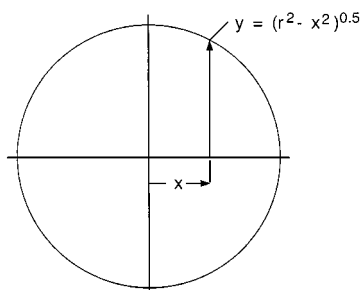
- L length of cylinder
- D diffusion coefficient
- c average speed = $(8kT/(\pi\mu))^{0.5}$
- δ mean collisional diameter = $0.5(\delta_1 + \delta_2)$
- μ reduced mass
- k Boltzmann constant.

B. Photochemistry

General considerations. All photolyses were carried out using an air-purged low-pressure mercury lamp with principal emissions at 185 and 254 nm. As the absorption coefficient of HC_3N at 254 nm is nearly 1000 times less than that at 185 nm, the photochemistry observed is the result of absorption of 185 nm photons.

The low mixing ratios used in the flow runs result in a very small number of photons being absorbed. In order to maximize the photon flux into the photolysis cell, irradiations were performed through the side of the cylindrical photolysis cell (Fig. 1). The path length through the cell varies as a function of where the light strikes the cell. In order to calculate the fraction of light absorbed in this configuration, a definite integral for the average value of a function was used (Fig. 2) (Salas *et al.* 1986).

Actinometry. Ammonia (NH_3) (Groth and Rommel 1965, Noyes and Leighton 1941) actinometry was used to determine lamp flux at 185 nm. Since the number of moles of gas present

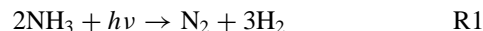


$$\frac{\int_0^{1.25} 1 \cdot 10^{-abc} dx}{\int_0^{1.25} dx}$$

where b = path length = function of position on circular cell = $2 \cdot y$
 r = radius of cell
 x = position on cell

FIG. 2. Calculation of fraction of light absorbed by the cell. (Top view of cell).

in the system increases as a result of photolysis (R1), the total pressure in the system rises during an irradiation. Therefore, measuring the extent of reaction requires only an accurate measurement of the system pressure. The increase in pressure at any time is equal to the loss of NH_3 for the same time. A static photolysis was performed in which a section of the flow line was filled with a quantity of NH_3 sufficient to absorb all the incident light (20 Torr), and the increase in pressure was recorded. Taking the quantum yield for NH_3 loss at 185 nm and 20 Torr as 0.28 (Groth and Rommel 1965) results in a flux of 1.16×10^{18} photons \cdot min $^{-1}$.



C. Analysis

HC_3N loss and product formation. NMR (Varian Unity 500) and FTIR (Perkin-Elmer 1800) spectroscopies were used for the determination of reactant loss and product formation. At the completion of a flow run, volatile products were transferred under vacuum to a gas IR cell (10 cm, NaCl windows) and spectra were taken at a resolution of 0.5 cm^{-1} . HCN was identified by comparison of its FTIR spectrum with that of an authentic sample. Comparison of peak areas at 3320 and 3351 cm^{-1} to standard curves was used for the determination of HC_3N loss and HCN formation, respectively. The gases were then transferred to a quartz cell and extracted into a weighed amount of CDCl_3 (Clarke and Ferris 1996). Acrylonitrile (CH_2CHCN) and acetonitrile (CH_3CN) were identified by comparison of their NMR spectra with authentic samples. The identification of CH_3CN was supported by measuring the NMR after adding an amount of CH_3CN equal to that formed to the CDCl_3 solution of the photoproducts. A single sharp peak at the chemical shift of CH_3CN was observed. The amount of CH_3CN formed was determined by comparing the integration of NMR signal at 2.010δ with the signal from the residual CHCl_3 in the CDCl_3 solvent. NMR signals at 5.671 , 6.072 , and 6.096δ were used for CH_2CHCN determinations.

Polymer. Polymer films were collected on a quartz plate resting on a quartz boat inserted in the side of the flow cell (Fig. 3). The infrared spectra of the film polymers were measured on samples scraped from the quartz plate and transferred to a NaCl in a Spectra Tech Spectra Scope infrared microscope attachment to the FTIR. Polymer powders were collected in a chamber (Fig. 3) connected to the bottom of quartz cell via an O-ring joint. The gas and polymer were constrained through a funnel and impinge on a scanning electron microscope (SEM) stub covered with aluminum foil on carbon tape. The constriction that resulted from pressing the tip of the funnel into the aluminum foil on the carbon tape allowed the particles to collect. The stub was then removed and SEM analyses (JEOL JSM-840) were performed as previously described (Clarke and Ferris 1997b).

Photolysis of propionitrile. Propionitrile (propanenitrile, Aldrich) was degassed on a vacuum line and shown to be pure

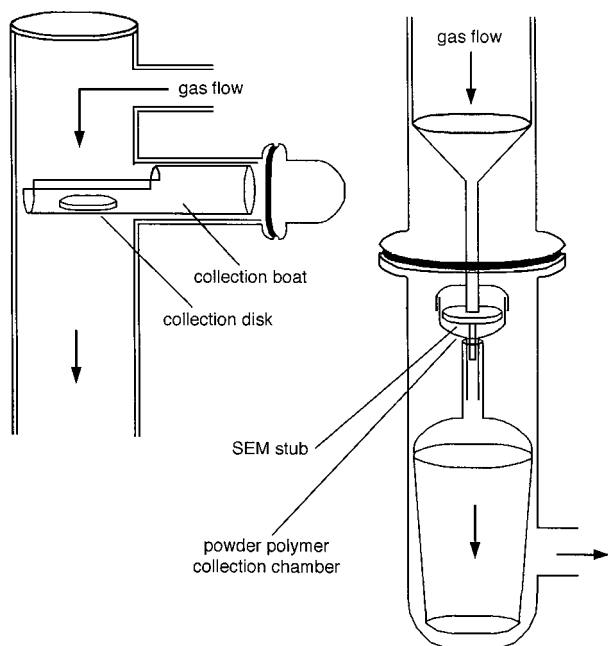


FIG. 3. Polymer film collection chamber (left) and polymer powder collection chamber (right).

by ^1H NMR. Two Torr was added to a 2.5×10 cm cylindrical quartz cell and irradiated for 4 h by the same low pressure mercury lamp used in the flow reactor. ^1H NMR analysis of the products was performed as described above.

RESULTS AND DISCUSSION

A. Flow System

The purpose of this research was to develop and evaluate the photochemical flow reactor using reactants of atmospheric interest. This approach was prompted by our previous laboratory investigations of the photochemistry on Titan using a static system. In the static approach it was not possible to duplicate the low mixing ratios of the minor atmospheric constituents (10^{-4} – 10^{-9}) which make important contributions to the atmospheric photochemistry (Clarke and Ferris 1997a). The lowest possible mixing ratio attainable in our static system, $\sim 10^{-3}$, is governed by the sensitivity of the pressure gauge used to prepare the reactant mixtures and by the sensitivity of the analytical methods available to determine the rates of reactant loss and the product formation. These limitations do not apply to flow systems. The reactant gases are measured at higher pressures and then diluted with an inert gas. The amount of reactant consumed is controlled by the flow rate through the system. At lower flow rates, the reactant gas remains in the reaction zone for a longer period of time (longer residence time), which results in an increased degree of conversion. The amount of product collected can be increased, not only by increasing the degree of conversion, but also by extending the length of time that the gases are flowed. In this research, gases were flowed from 7–13 h at a rate

of 15 standard cubic centimeters per min (15 sccm). This flow rate resulted in a residence time of 15.8 min in the photolysis cell and a percentage of conversion to products of less than 5%.

The light source used in the flow reactor is a low-pressure mercury vapor lamp with principal emissions of 185 and 254 nm of radiation. UV light was chosen as the energy source because solar ultraviolet light is the predominant energy source driving the atmospheric chemistry on Titan (Clarke and Ferris 1997a, Sagan and Thompson 1984). A 185-nm light source was used to simulate the photochemistry initiated by the longer wavelength UV that is not absorbed by methane but is absorbed by the unsaturated compounds present on Titan. In addition, the solar photon flux at the longer wavelengths is greater than at shorter wavelengths. Photochemical reactions more closely simulate the atmospheric chemistry occurring on Titan than electrical or plasma discharge studies (Sagan *et al.* 1992, McDonald *et al.* 1994, Thompson *et al.* 1991, 1994).

The flow reactor has four important advantages over static systems in the laboratory simulations of the atmospheric photochemistry of Titan or atmospheres of other bodies. First, measurable amounts of minor constituents can be mixed with a large amount of a carrier gas, nitrogen in the case of Titan, to obtain the mixing ratios that approximate those in the atmosphere being investigated (Table II). As noted above, a second advantage is that one can vary the flow time and flow rate to obtain enough products for analysis. The third advantage is that the composition of the gas mixture being photolyzed does not change with time because fresh reactant gas is always passing through the flow cell. This is a much better model of a planetary atmosphere than a static system because usually only a small percentage of the total atmosphere is undergoing photolysis at any one time. In addition, the gas flow removes the initial photoproducts from the irradiation zone and thus minimizes the formation of secondary photoproducts. Fourth, the very low partial pressures of the reactants results in their absorption of less than 1% of the incident light. This results in photochemistry throughout the volume of the irradiation chamber and not just near its walls. This, together with the high pressure of inert gas, minimizes the possibility that reactions on the walls could give reaction products that would not be observed in the planetary atmosphere being studied.

There are two limitations of a photochemical flow system. The first arises in the preparation of the reactant mixture. Currently, the best quality nitrogen available is 99.9999% pure. The impurities present in the gas have a total mixing ratio of 10^{-6}

TABLE II
Comparison of Reaction Conditions to Those on Titan

	Titan	Static experiments	Flow experiments
Total pressure (Torr)	7.6–76	1–760	700
Mixing ratio			
HC_3N	10^{-7} – 10^{-9}	1 – 10^{-3}	10^{-3} – 10^{-6}
N_2	0.98	0–0.99	1.0

TABLE III
ULSI Nitrogen (99.9999%)

Impurity	Our tank ^a (mixing ratio)
Oxygen	1×10^{-7}
Carbon dioxide	$<1 \times 10^{-7}$
Carbon monoxide	$<1 \times 10^{-7}$
Total hydrocarbon content	$<1 \times 10^{-7}$
Water	1×10^{-7}

^a As per Certificate of Analysis (Lot G38-1102-C4) provided by Matheson (Montgomeryville, PA).

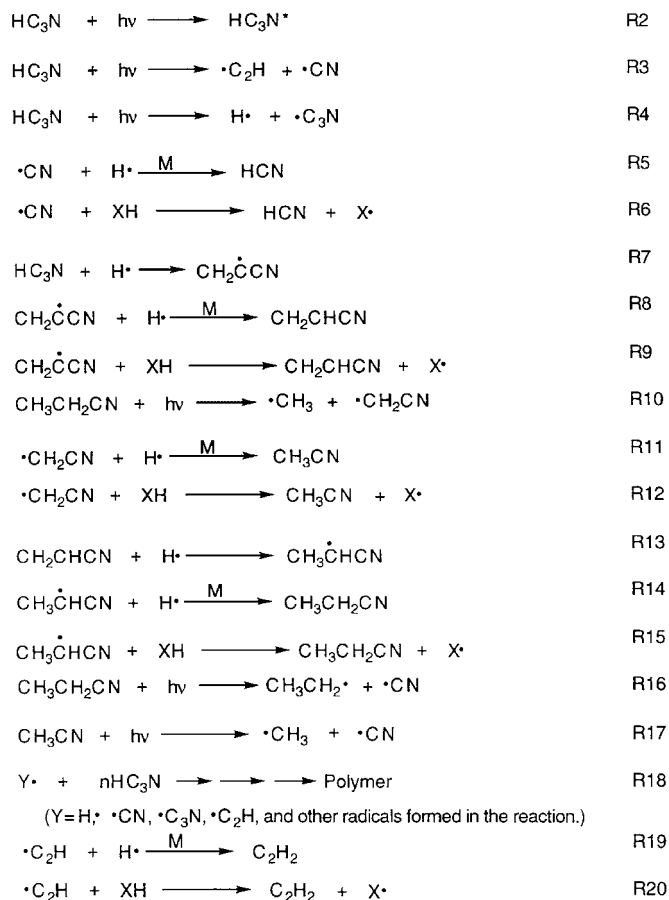
(Table III). Consequently, one cannot use reactant mixing ratios of less than 10^{-6} , and additional care must be exercised in interpreting the results of experiments with mixing ratios that approach this value. The absence of significant variation in the quantum yields between experiments with high reactant mixing ratios and those with low reactant mixing ratios, where the impurities represent a smaller proportion of the reactants, would suggest that impurity problems were not significant in this study. The lack of these variations is evident in the following discussions of quantum yields, polymer morphology, and polymer FTIR spectra. The second limitation is the low fraction of light absorbed by the reactant gas. This is determined by both the mixing ratio of the absorbing gas and the total pressure in the system. Currently, the system is operated at HC_3N mixing ratios between 10^{-3} and 10^6 and a total pressure of 700 Torr. This results in absorption of only between 1.7×10^{-1} and $2.5 \times 10^{-3}\%$ of the incident light or between 2.0×10^{15} and 2.9×10^{13} photons $\cdot \text{min}^{-1}$, respectively. Consequently, further lowering of the mixing ratios or the operating pressure is not possible as the resulting photolysis time required would be too long to be practical. Hence it was not possible to operate the flow system at the approximate pressure (7.6 Torr) and temperature (160 K) where light of wavelengths greater than 160 nm is reaching HC_3N in the stratosphere of Titan. The flow system will have to be modified to carry out photolyses at 160 K, the temperature in Titan's stratosphere, rather than at 298 K. We do not believe temperature will be an important factor in these studies because the photon energy is dependent on its frequency and not on the ambient temperature. Low-temperature studies will be undertaken since temperature influences the rates of subsequent thermal reactions.

B. HC_3N Photolysis

The simulated Titan photochemical reactions we performed in static systems, with higher partial pressures of reactant gases, laid the groundwork for the flow reaction studies (Yung *et al.* 1984, Clarke and Ferris 1997b). Mixtures of HC_3N and N_2 were used in this initial study to test the flow system and to provide baseline data for the reaction of gas mixtures which more accurately model the mixture of gases in Titan's stratosphere. The mixing ratios of HC_3N used in the flow studies were varied in decades from 10^{-4} to 10^{-6} . Mixing ratios of HC_3N lower

than 10^{-6} were avoided because the sum of the mixing ratios of the impurities in the N_2 used is in the 10^{-7} – 10^{-6} range (Table III). The identities and yields of gaseous products, HCN, CH_3CN , and CH_2CHCN , and the amount of unreacted HC_3N were determined by quantitative proton nuclear magnetic resonance spectroscopy (^1H NMR) and Fourier transform infrared spectroscopy (FTIR). These quantitative data together with the measurement of the lamp's flux at 185 nm permitted the calculation of quantum yields. The structural units present in the polymeric products formed were determined from their FTIR spectra. The quantum yields of reactant loss and product formation, along with the degree of incorporation of the starting material into the polymer, made it possible to propose an overall description of the photochemical reaction pathway.

Quantum yields. The photolysis of gas mixtures containing 700 Torr of an $\text{N}_2 : \text{HC}_3\text{N}$ mixture with HC_3N mixing ratios ranging from 10^{-4} to 10^{-6} resulted in the consumption of HC_3N and the formation of HCN, CH_3CN , CH_2CHCN , and a solid (polymeric) product. The initial steps in the photolysis of HC_3N are given in (R2)–(R4) in Scheme 1. The quantum yields determined for the loss of HC_3N (Table IV) are consistent with the quantum yields obtained in the static system (Clarke and Ferris 1996). The



SCHEME 1

TABLE IV
Quantum Yields for Photochemical Static and Flow Reactions of HC₃N

Reaction type	Mole fraction HC ₃ N	HC ₃ N pressure (Torr)	QY HC ₃ N loss	QY HCN formation	QY CH ₃ CN formation	QY CH ₂ CHCN formation	QY 1,3,5,TCB formation
Static	1	25.0	0.61	ND	ND	ND	0.009
Static	1	17.5	0.47	ND	ND	ND	0.006
Static	1	10.0	0.38	ND	ND	ND	0.003
Static	1	5.0	0.32	ND	ND	ND	0.001
Static	1	2.5	0.31	ND	ND	ND	ND
Static	1	1.0	0.35	ND	ND	ND	ND
Flow	1.7×10^{-4}	7.0×10^{-2}	1.18	0.28	1.1×10^{-2}	0.01	ND
Flow	1.7×10^{-5}	7.0×10^{-3}	2.44	1.29	4.9×10^{-2}	ND	ND
Flow	1.7×10^{-6}	7.0×10^{-4}	2.78	1.76	5.6×10^{-2}	ND	ND

Note. QY, quantum yield; ND, not detected; TCB, tricyanobenzene.

quantum yields in the static system decrease with the decreasing of HC₃N pressure from 25 to 2.5 Torr and then increase in the 2.5 to 1.0 Torr range. At the lower pressures used in the flow system, the quantum yield for HC₃N loss continues to increase as the pressure is further decreased to 7.0×10^{-4} Torr (10^{-6} mixing ratio) (Table IV). As expected from the decreasing quantum yields in the static system, no 1,3,5-tricyanobenzene was found in any of the flow runs. The formation of HCN, CH₃CN, or CH₂CHCN observed in the flow runs was not observed in the static reactions.

The quantum yields for the formation of HCN and CH₃CN increase as the mixing ratio of HC₃N is decreased (Table IV). These increases suggest that the rate of HCN and CH₃CN formation increases relative to the rate of polymer formation as the pressure of HC₃N decreases.

HCN, the primary non-polymeric product, is formed by the reaction of the ·CN (R5 and/or R6) formed in (R3). The proportional increases in the quantum yields for HC₃N loss and HCN formation are coupled as would be expected if ·CN were produced by (R3). It is not clear why the quantum yields for HCN formation are greater than one, an indication of a chain reaction. The formation of CH₂CHCN would be expected from H· addition to HC₃N (R7) followed by reaction (R8) or (R9).

The formation of CH₃CN, a minor product, from the photolysis HC₃N was initially puzzling and was investigated further. One possible pathway is via the photolysis of propionitrile (CH₃CH₂CN) (R10). CH₃CH₂CN can be formed in the reaction mixture by the reduction of CH₂CHCN, (R13)–(R15). We found that irradiation of CH₃CH₂CN yielded HCN and CH₃CN in a ratio of 5.6 : 1, respectively. Observation of CH₃CN indicates the ·CH₂CN radical, resulting from the photochemical β-cleavage of CH₃CH₂CN (R10), yields CH₃CN by (R11) and/or (R12).

HCN formation proceeds by the α-cleavage of CH₃CH₂CN (R16) to give ·CN, which yields HCN by radical combination (R5) or abstraction (R6). HCN formation appears to be a general reaction of alkyl nitrile photolysis (R16) since HCN is also formed from photolysis of CH₃CN (R17) (McElcheran *et al.* 1958). Photolysis of the nitrile intermediates leading to

the formation of polymeric products may be the source of some of the HCN produced in the flow reactions. This may also explain why the intensity of the nitrile absorption (2210 cm^{-1}) in the FTIR spectrum decreases in the polymeric products as the mixing ratio of the starting HC₃N decreases (Fig. 4) and the quantum yield of HCN formation increases (Table IV).

Polymer formation. Polymer formation was studied at HC₃N mixing ratios of 10^{-3} to 10^{-6} . It is initiated by excited state HC₃N (R2) and by the radicals formed from the photodissociation of HC₃N, (R3) and (R4), to give polymer, (R18) (Clarke and Ferris 1995). Polymer is the principal reaction product in experiments with HC₃N mixing ratios greater than 10^{-4} while HCN predominate at mixing ratios less than 10^{-4} . Since no C₂H₂ was observed as a reaction product, the polymer is most likely a copolymer of HC₃N and ·C₂H. The similarity of the reactions that produce C₂H₂ (R3, R19, and/or R20) to those producing HCN (R3, R5, and/or R6) would predict that the amount of C₂H₂ formed should equal the amount of HCN formed.

The empirical formula of the polymer can be estimated from the reaction products observed (Table V). The moles of H, C, and N in the HC₃N consumed minus the moles of H, C, and N

TABLE V
C–H–N Ratios in Polymers Generated in HC₃N Flow Reactions

Mixing ratio of HC ₃ N	10^{-4}	10^{-5}	10^{-6}
HC ₃ N consumed (mol/min)	4.2×10^{-9}	8.0×10^{-10}	1.4×10^{-10}
HCN produced (mol/min)	1.1×10^{-9}	4.2×10^{-10}	8.6×10^{-11}
CH ₂ CHCN produced (mol/min)	5.1×10^{-11}	0	0
CH ₃ CN produced (mol/min)	1.7×10^{-10}	1.6×10^{-11}	2.7×10^{-12}
H incorporated into polymer (mol/min)	2.5×10^{-9}	3.3×10^{-10}	4.2×10^{-11}
C incorporated into polymer (mol/min)	1.6×10^{-6}	2.8×10^{-7}	4.6×10^{-8}
N incorporated into polymer (mol/min)	5.8×10^{-7}	7.0×10^{-8}	9.2×10^{-9}
Empirical formula	H _{1.0} C _{4.4} N _{1.2}	H _{1.0} C _{5.9} N _{1.1}	H _{1.0} C _{7.6} N _{1.1}

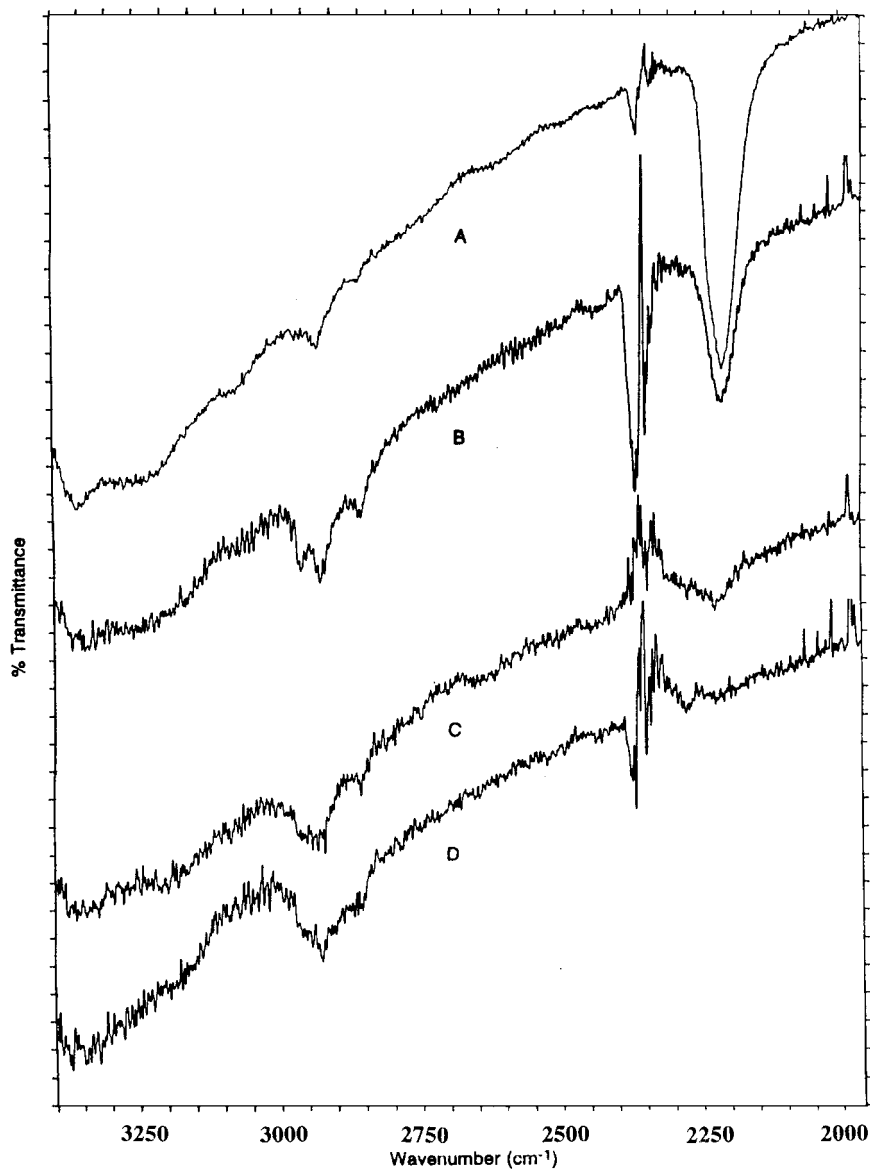


FIG. 4. FTIR spectra for the polymeric materials generated in the $N_2 : HC_3N$ flow reaction series. (A) 10^{-3} MR, (B) 10^{-4} MR, (C) 10^{-5} MR, (D) 10^{-6} . The peaks between 2290 and 2400 cm^{-1} are due to atmospheric CO_2 .

in the non-polymeric products formed equals the moles of the H, C, and N in the polymer. The polymer has approximately a 1 : 1 H : N ratio at all mixing ratios while the C : H ratio increases from 4.4 to 7.6 as the HC_3N mixing ratio decreases from 10^{-4} to 10^{-6} .

FTIR analysis. The polymers formed from the irradiation of HC_3N at mixing ratios of 10^{-3} to 10^{-6} were removed from the photolysis cell, and the infrared spectra were measured (Fig. 4). The spectrum of the polymer formed at a 10^{-3} mixing ratio of HC_3N was comparable to that of the polymers prepared by the static irradiation of HC_3N (Clarke and Ferris 1996). Peaks could be assigned to N–H (3330 cm^{-1}), C–H in CH_3 (2960 and 2870 cm^{-1}), C–H in CH_2 (2920 and 2854 cm^{-1}), and $C\equiv N$

(2210 cm^{-1}). Unlike with the static polymer, no peaks due to the triple bond ($C\equiv C$) at 2100 cm^{-1} (Silverstein *et al.* 1981) were observed.

A marked decrease in the intensity of the nitrile stretching frequency (2210 cm^{-1}) was observed as the mixing ratio of HC_3N was decreased (Fig. 4). This finding is consistent with the decrease in the nitrogen content of the polymer relative to carbon (Table V). The observation of an N–H stretching frequency at 3300 cm^{-1} and the very weak nitrile stretch at 2210 cm^{-1} in the polymers formed at the 10^{-5} and 10^{-6} mixing ratios suggest that the decrease may be due to the reduction of the nitrile group to an amino group. This conclusion is consistent with the formation of ammonia (NH_3) by pyrolysis of the polymer formed in a static system (Clarke and Ferris 1997a). The presence of infrared

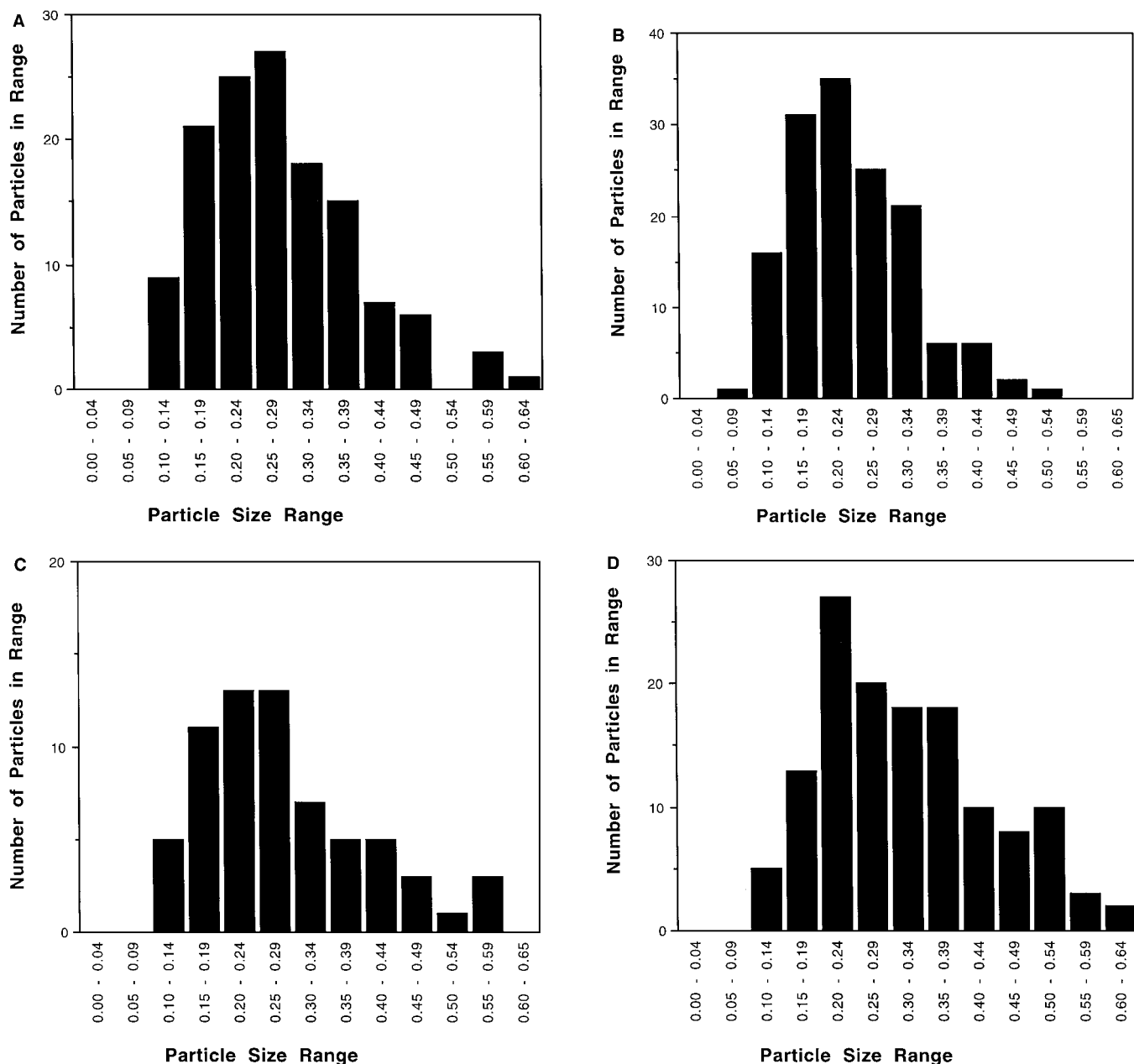


FIG. 5. Particle size distributions for the polymeric materials generated in the $\text{N}_2:\text{HC}_3\text{N}$ flow reaction series. Particle size range is in micrometers. (A) 10^{-3} MR, (B) 10^{-4} MR, (C) 10^{-5} MR, (D) 10^{-6} .

absorption due to CH_3 and CH_2 groupings is also consistent with reduction processes which result in the formation of polymer chains with terminal CH_3 groupings and internal CH_2 groupings.

The particle size and morphology of the polymer were determined from SEM images (Fig. 5). The morphology and appearance of particles formed in the $\text{N}_2:\text{HC}_3\text{N}$ series of flow reactions are quite similar to those generated in static irradiations of HC_3N (Clarke and Ferris 1997b). Particle size distributions for the polymer were measured for each mixing ratio of HC_3N studied, with the majority of particles falling between

0.15 and 0.34 μm in diameter. A similar particle size distribution was observed for the HC_3N polymer generated in static irradiation reactions with 50 Torr of HC_3N , which ranged from 0.1 to 0.7 μm in diameter (Clarke and Ferris 1997b). The particle size does not vary significantly with the partial pressure of the HC_3N or the mode (static or flow) of irradiation of the gas mixture. These results compare favorably to other studies of Titan haze, where high pressures of a variety of gas mixtures and either ultraviolet light or an electrical discharge were used as the energy source; polymers were produced with particle sizes

ranging from 0.10–1.18 μm (Bar-Nun *et al.* 1988, Scattergood *et al.* 1992). While the HC_3N particles have sizes comparable to those of the Titan haze (Tomasko and Smith 1982, West *et al.* 1983, Rages and Pollack 1983), it is highly unlikely that particles made from the irradiation of pure HC_3N are present on Titan. The particles and material, which constitute the haze on Titan, are formed by the photolysis of mixtures of HC_3N with other Titan gases. However, these results demonstrate that photochemical processes are able to produce particles of appropriate size at mixing ratios similar to those found on Titan.

CONCLUSIONS

Since ultraviolet light is the major source of energy for a majority of planetary atmospheric reactions, and certainly those in Titan's atmosphere, the use of ultraviolet radiation allows for a more realistic laboratory simulation than the use of a plasma discharge. The successful use of a photochemical flow reactor for the investigation of the volatiles and solids produced by HC_3N photolysis indicates that it is now possible to simulate atmospherically important photochemical processes. To date, this is the only system capable of preparing, photolyzing, and analyzing gas mixtures at mixing ratios truly representative of the gas mixtures found in planetary atmospheres. The extended reaction times possible with a flow reactor makes collection of products possible. Once collected, any number of methods, including NMR, FTIR, SEM, and mass spectrometry, can be used to analyze these products. The quantitative data obtained using this approach is able to provide information about the structure and rate of formation of photoproducts that are directly applicable to the planet or moon of interest.

The quantum yields and polymer analyses obtained in this research provide insight into the composition of the haze generated photochemically in Titan's stratosphere. The quantum yields for HCN and CH_3CN formation (Table IV) demonstrate that the nitrogen of HC_3N is not incorporated into the Titan haze in appreciable amounts. This is shown quantitatively by the high C/N ratio in the polymer as the HC_3N mixing ratio is decreased (Table V). This conclusion is confirmed by the infrared spectra of the polymer in which the intensity of the $\text{C}\equiv\text{N}$ stretching frequency decreases as the HC_3N mixing ratio is lowered to a mixing ratio closer to that of Titan (Fig. 4). It is predicted from the empirical formulas in Table V that the C/N ratio of Titan's stratospheric haze, measured by the Huygens probe, will be much higher than the C/N ratio of gases present in Titan's atmosphere. The quantum yields (rates) and reaction pathways determined in this study will be applicable to modeling the atmospheric chemistry of Titan.

ACKNOWLEDGMENTS

This research was supported by NASA grant NAG5-4557, NASA NSCORT grant NAG5-7598, and a NASA Graduate Researcher's Award to David W. Clarke. The valuable assistance of Dr. Herbert Schwartz with the NMR and FTIR analyses is appreciated.

REFERENCES

- Bamford, C. H., and C. S. H. Tipper 1969. *Comprehensive Chemical Kinetics*. Elsevier, Amsterdam.
- Bar-Nun, A., I. Kleinfeld, and E. Ganor 1988. Shape and optical properties of aerosols formed by photolysis of acetylene, ethylene and hydrogen cyanide. *J. Geophys. Res.* **93**(D7), 8383–8387.
- Clarke, D. W., and J. P. Ferris 1995. Photodissociation of cyanoacetylene: Application to the atmospheric chemistry on Titan. *Icarus* **115**, 119–125.
- Clarke, D. W., and J. P. Ferris 1996. Mechanism of cyanoacetylene photochemistry at 185 and 254 nm. *J. Geophys. Res. Planets* **101**, (E3), 7575–7584.
- Clarke, D. W., and J. P. Ferris 1997a. Chemical evolution on Titan: Comparisons to the prebiotic Earth. *Origins Life Evol. Biosphere* **27**(1–3), 225–248.
- Clarke, D. W., and J. P. Ferris 1997b. Titan haze: Structure and properties of cyanoacetylene and cyanoacetylene–acetylene photopolymers. *Icarus* **127**, 158–172.
- Coustenis, A., A. Salama, E. Lellouch, Th. Encrenaz, G. L. Bjoraker, R. E. Samuelson, Th. de Graauw, H. Feuchtgruber, and M. F. Kessler 1998. Evidence for water vapor in Titan's atmosphere from ISO/SWS data. *Astron. Astrophys.* **336**, L85–L89.
- Ferris, J. P., and J. C. Guillemin 1990. Photochemical cycloaddition reactions of cyanoacetylene and dicyanoacetylene. *J. Org. Chem.* **55**, 5601–5606.
- Ferris, J. P., R. A. Sanchez, and L. E. Orgel 1968. Studies in prebiotic synthesis III. Synthesis of pyrimidines from cyanoacetylene and cyanate. *J. Mol. Biol.* **33**, 693–704.
- Ferris, J. P., O. S. Zamek, A. M. Altbuch, and H. Freiman 1974. Chemical evolution XVIII. Synthesis of pyrimidines from guanidine and cyanoacetaldehyde. *J. Mol. Evol.* **3**, 301–308.
- Groth, W., and H. J. Rommel 1965. Photochemische untersuchungen im Schumann-Ultraviolett Nr. 12: Die photolyse des ammoniks bei dem wellenlangen 1849 Å (Hg), 1470 Å (Xe), 1236 und 1165 Å (Kr). *Z. Phys. Chem. Neue Folge* **45**, 96–116.
- Halpern, J. B., G. E. Miller, H. Okabe, and W. Nottingham 1988. The UV photochemistry of cyanoacetylene. *J. Photochem. Photobiol. A* **42**, 63–72.
- Halpern, J. B., G. E. Miller, and H. Okabe 1989. The reaction of CN radicals with cyanoacetylene. *Chem. Phys. Lett.* **155**(4–5), 347–350.
- Halpern, J. B., L. Petway, R. Lu, W. M. Jackson, and V. R. McCrary 1990. Photochemistry of cyano- and dicyanoacetylene at 193 nm. *J. Phys. Chem.* **94**, 1869–1873.
- Job, V. A., and G. W. King 1966a. The electronic spectrum of cyanoacetylene Part I. Analysis of the 2600 Å band system. *J. Mol. Spectrosc.* **19**, 155–177.
- Job, V. A., and G. W. King 1966b. The electronic spectrum of cyanoacetylene Part II. Analysis of the 2300 Å band system. *J. Mol. Spectrosc.* **19**, 178–184.
- Kuiper, G. P. 1944. Titan: A satellite with an atmosphere. *Astrophys. J.* **100**, 378–383.
- McDonald, G. D., W. R. Thompson, M. Heinrich, B. Khare, and C. Sagan 1994. Chemical investigation of Titan and Triton tholins. *Icarus* **108**, 137–145.
- McElcheran, D. E., M. H. Wijnen, and F. W. Steacie 1958. The photolysis of methyl cyanide at 1849 Å. *Can. J. Chem.* **36**, 324–329.
- Miller, F. A., and D. H. Lemmon 1967. The infrared and Raman spectra of dicyanodiacetylene (NCCCCCN). *Spectrochim. Acta* **23A**, 1415–1423.
- Moureaux, C., and J. C. Bongrand 1920. Le cyanoacetylene C_3NH . *Ann. Chem. Paris* **14**, 47–58.
- Noyes, W. A., Jr., and P. A. Leighton 1941. *The Photochemistry of Gases*, p. 475. Dover, New York.
- Rages, K., and J. B. Pollack 1983. Vertical distribution of scattering hazes in Titan's upper atmosphere. *Icarus* **55**, 50–62.
- Sagan, C., and W. R. Thompson 1984. Production and condensation of organic gases in the atmosphere of Titan. *Icarus* **59**, 133–161.

- Sagan, C., W. R. Thompson, and B. N. Khare 1992. Titan: A laboratory for prebiological organic chemistry. *Acc. Chem. Res.* **25**, 286–292.
- Salas, S. L., E. Hille, and J. T. Anderson 1986. *Calculus: One and Several Variables*, 5th ed., pp. 287–290. Wiley, New York.
- Scattergood, T. W., E. Y. Lau, and B. M. Stone 1992. Titan's aerosols. *Icarus* **99**, 98–105.
- Seki, K., M. He, R. Liu, and H. Okabe 1996. Photochemistry of cyanoacetylene at 193.3 nm. *J. Phys. Chem.* **100**, 5349–5353.
- Silverstein, R. M., G. C. Bassler, and T. C. Morrill 1981. *Spectrophotometric Identification of Organic Compounds*, 4th ed. Wiley, New York.
- Thompson, W. R., T. J. Henry, J. M. Schwartz, B. N. Khare, and C. Sagan 1991. Plasma discharge in N_2 - CH_4 at low pressures: Experimental results and applications to Titan. *Icarus* **90**, 57–73.
- Thompson, W. R., G. D. McDonald, and C. Sagan 1994. The Titan haze revisited: Magnetospheric energy sources and quantitative tholin yields. *Icarus* **112**, 376–381.
- Tomasko, M. G., and P. H. Smith 1982. Photometry and polarimetry of Titan: Pioneer 11 observations and their implications for aerosol properties. *Icarus* **51**, 65–95.
- West, R. A., A. L. Lane, H. Hart, K. E. Simmons, C. W. Hord, D. L. Coffeen, W. Esposito, M. Sato, and R. B. Pomphrey 1983. Voyager 2 photopolarimeter observations of Titan. *J. Geophys. Res.* **88**, 8688–8708.
- Yung, Y. L., M. Allen, and J. P. Pinto 1984. Photochemistry of the atmosphere of Titan: Comparison between model and observations. *Astrophys. J. Suppl. Ser.* **55**, 465–506.